Retrosynthesis Prediction using Grammar-based Neural Machine Translation: An Information-Theoretic Approach

Vipul Mann, Venkat Venkatasubramanian*

Department of Chemical Engineering, Columbia University, New York, NY, 10027, USA

Abstract

Retrosynthetic prediction is one of the main challenges in chemical synthesis that requires identifying reaction pathways and precursor molecules for synthesizing a target molecule. This requires a search over the space of plausible chemical reactions that often results in complex, multi-step, branched synthesis trees for even moderately complex organic reactions. Here, we propose an approach that performs single-step retrosynthesis prediction using SMILES grammar-based representations in a neural machine translation framework. Information-theoretic analyses of such grammar-representations reveal that they are both superior and well-suited for machine learning tasks due to their underlying redundancy and high information capacity compared to purely character-based representations. We report the top-1 prediction accuracy of 43.8% (top-5 measure of 61.4%) and syntactic validity of 95.6% (top-5 measure of 91.6%) on a standard reaction dataset. Comparing our model's performance with previous work that used purely character-based SMILES representations demonstrate improved accuracy and reduced grammatically invalid predictions.

Keywords: Retrosynthesis prediction; Computer-aided synthesis planning; Sequence-to-sequence models; Information theory; Transformer

1. Introduction

One of the important challenges in computational chemistry is the retrosynthetic analysis of desired molecules that satisfy property constraints, subject to the commercial availability of the precursors involved and the feasibility of the chemical reactions required for their synthesis. The immense interest in this problem over the recent years could be attributed to its practical applications across areas such as drug discovery, synthesis of novel organic compounds, and improvements in

---

*Corresponding author

Email addresses: `vm2583@columbia.edu` (Vipul Mann), `venkat@columbia.edu` (Venkat Venkatasubramanian)

the reactions pathways from a commercial, social, or economic viability standpoint. The industrial applications of retrosynthetic analysis include automobiles, petrochemicals, specialty chemicals, and polymer science, with a great potential to revolutionize the entire industry if the right compound could be synthesized.

Retrosynthetic analysis often involves evaluating a large number of potential candidate reaction pathways and molecules at multiple stages of the reaction resulting in complex retrosynthesis trees that need to be searched and parsed efficiently. Computational approaches could significantly aid the chemist in solving different aspects of the retrosynthesis problem, such as the graph-theoretic search methodologies for efficient tree traversal for the identification of feasible reaction pathways, dictionary-based methods combined with heuristics for quicker evaluation of a combinatorially large search-space of precursors, and faster elimination of practically infeasible routes through chemistry-driven quantitative and qualitative heuristics. One of the first attempts that leveraged computational tools and formalized the retrosynthesis problem was LHASA, [1] which incorporated chemistry rules through logic and heuristics and developed a chemical programming language. Several subsequent approaches were proposed that utilized rule-based expert-systems [2, 3, 4, 5, 6, 7, 8, 9, 10, 11]. However, such approaches were hard to scale beyond interesting prototypes as they required great human effort and expertise to develop.

However, in recent years, the huge surge in computational capabilities combined with great advances in machine learning have resulted in a renewed attack on this problem. This includes approaches that combine neural network models with known chemistry knowledge encoded in the form of reaction templates – e.g., Segler and Waller [12] leveraged neural networks for selecting the reactivity centers and most suitable transformations; Wei et al. [13] predicted reaction types and used Smiles Molecular Arbitrary Target Specification (SMARTS) templates for predicting the likely products given a set of reactants and reagents, and Coley et al. [14] proposed selecting the suitable edit-based transformations in a reaction using reaction templates. Such methods, however, again address only certain limitations of the rules-based systems and the inherent limitation of the lack of their ability to suggest novel chemical reactions and a bias towards the common reaction types still exists.

This is overcome in purely data-driven approaches that use sophisticated machine learning architectures to learn the complex non-linear dynamics of a chemical reaction – both in the forward and

the backward directions – primarily through modeling the chemical representations. This includes the neural sequence-to-sequence (or seq2seq) models introduced for the forward reaction prediction in [15] and the retrosynthetic prediction in [16] that formulate the reaction prediction task as a sequence modeling problem. Other recent efforts for the retrosynthesis task include a seq2seq approach combined with a Monte Carlo tree search [17] and various transformer model-based approaches [18, 19, 20, 21, 22].

Even though the prediction accuracy has significantly improved owing to the increase in complexity of model architectures, the incorporation of prior chemistry knowledge in such frameworks is still lacking. The incorporation of this knowledge should, in principle, improve the model performance on out-of-sample examples. All the works in this area work with SMILES representations of molecules, treating them as merely character-based strings, except for the recent work by Ucak et al. [23] that uses substructure-based representations but suffers from lower prediction accuracy. In our earlier work on forward prediction [24, 25], we demonstrated that incorporating chemical and structural information about molecules ensures that the model learns the underlying chemical transformation using a model with significantly less number of training parameters. As an extension of that work, we propose here a framework for solving the retrosynthesis problem using the rich SMILES grammar-based representation of molecules and highlight the inherent benefits of such representations – both from an information-theoretic and model performance standpoint.

The rest of the paper is organized as follows: In Section 2, we formally define the retrosynthesis prediction problem as a sequence modeling task in the machine translation framework and present an overview of the methods underlying our work, such as the SMILES grammar, the transformer architecture and the beam search decoding procedure in Section 3. In Section 4, we present an information-theoretic analysis of the proposed grammar-representations and contrast them with the other representations (SMILES and molecular formula) to highlight the differences and quantify the advantages of using the underlying chemical structural information. The standard reaction dataset and the model training aspects of our work are presented in Section 5. The evaluation metrics used for assessing our model's performance, the results on the USPTO 50K reactions dataset, comparison with other works, and the limitations and future work in this direction are presented in Section 6. Finally, the concluding remarks summarizing our work's major contributions appear in Section 7.

2. Problem formulation and objectives

We formulate the retrosynthesis prediction problem as a sequence modeling task and use a machine translation framework for predicting the precursors for a given target molecule. The objective is to translate a set of input tokens corresponding to the product molecule to an output sequence of tokens corresponding to the precursor molecules. The input sequence is prepended with an identifier that indicates the reaction class that should be used to synthesize the given target molecule. In order to allow the model to differentiate between the different precursors (reactants), a separate identifier token is used to indicate the end of the representation of a given precursor and the start of another. This framework is depicted in Figure 1.
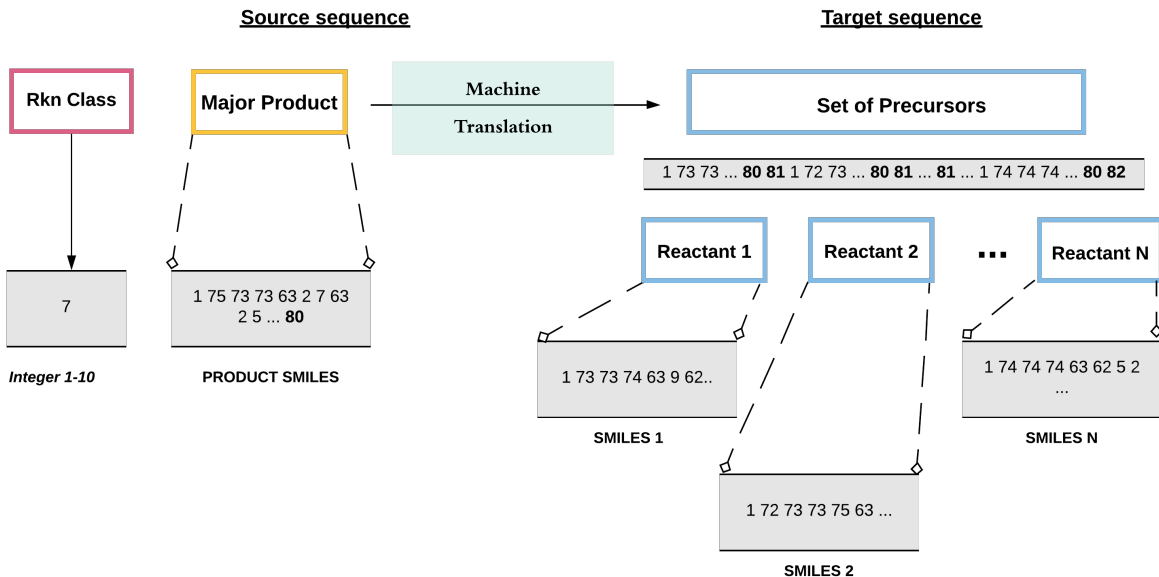

Figure 1: The single-step retrosynthesis prediction problem formulation using machine translation

In this framework, the participating product and reactants in a given reaction are represented using their corresponding grammar-based representation described in detail in Section 3.1. The representation starts with the token '1' and ends with the token '80' for all the molecules, the token '81' separates multiple reactants, and the token '82' signifies the end of all the precursor representations. The other identifiers (or tokens) correspond to the sequence of production rules required to obtain the given SMILES string, using the grammar productions described in Table 13 in the Appendix. The sequence modeling task is performed using a transformer model, a state-of-the-art architecture for sequence modeling, proposed in [26].

4

3. Methods

In this section, we describe the methods involving our approach, namely the SMILES grammar-based representations used for encoding molecules, the transformer architecture used for the sequence modeling task, and the beam search decoding procedure used for generating a set of most likely target sequences for a given input sequence.

3.1. SMILES grammar

One of the first works that attempted to formalize natural language through context-free grammars (CFGs) was proposed by Noam Chomsky [27] that was based on the idea that a group of words could be thought of as belonging to a constituent unit and that different constituent units could be grouped, hierarchically, to convey a given meaning. Formally, a context-free grammar could be thought of as a set of production rules that define the transformation of a set of non-terminal symbols to terminal symbols that correspond to strings with meaning in the natural language. In addition, there is a designated start symbol that indicates the start of a sentence. Therefore, a CFG consists of the following elements: S, a designated start symbol; Σ, the set of terminal symbols; N, the set of non-terminal symbols; and R, the set of production rules of the form A $\longrightarrow \beta$ where A $\in$ N is non-terminal and $\beta \in \Sigma$ is a terminal symbol.

A similar grammar for the SMILES representation of molecules also exists [28] where the individual tokens in the SMILES string represent the terminal symbols that could be obtained through the sequential application of a set of production rules on the non-terminal symbols. Consider, for example, a subset of the official SMILES grammar presented in Table 1. The equivalent symbols similar to CFG for this grammar are:

- S: `SMILES`

- Σ: { `(`, `)`, `=`, `c`, `C`, `O`, `1`, `2` }

- N: { `SMILES`, `CHAIN`, `BRANCHED_ATOM`, `BOND`, `ATOM`, `RINGBOND`, `BB`, `RB`, `BRANCH`, `AROMATIC_ORGANIC`, `ALIPHATIC_ORGANIC`, `DIGIT` }

- R: productions (rules) 1 through 20 in Table 1

Table 1: Reduced SMILES grammar

S.No	Production rules
1	SMILES ⟶ CHAIN
2	CHAIN ⟶ CHAIN BRANCHED_ATOM
3	CHAIN ⟶ CHAIN BOND BRANCHED_ATOM
4	CHAIN ⟶ BRANCHED_ATOM
5	BRANCHED_ATOM ⟶ ATOM RINGBOND
6	BRANCHED_ATOM ⟶ ATOM
7	BRANCHED_ATOM ⟶ ATOM BB
8	BRANCHED_ATOM ⟶ ATOM RB
9	BB ⟶ BRANCH
10	RB ⟶ RINGBOND
11	BRANCH ⟶ (CHAIN)
12	RINGBOND ⟶ DIGIT
13	BOND ⟶ =
14	ATOM ⟶ AROMATIC_ORGANIC
15	ATOM ⟶ ALIPHATIC_ORGANIC
16	AROMATIC_ORGANIC ⟶ c
17	ALIPHATIC_ORGANIC ⟶ C
18	ALIPHATIC_ORGANIC ⟶ O
19	DIGIT ⟶ 1
20	DIGIT ⟶ 2

We leverage such underlying grammar to assign structure to a given SMILES string and derive from such structures the grammar-based representations. Consider benzene, with the SMILES string representation given by C1=CC=CC=C1. This representation could be obtained by applying the set of production rules in Table 1 sequentially to obtain the corresponding parses-tree shown in Figure ??. The grammar-representation that we work with, originally proposed in our earlier work [24], is obtained by extracting production rules from the parse-tree by parsing it in a bottom-up-left-corner strategy, i.e., starting at the top and going down the left-most branch, then coming back up to parse the immediate right branch, and so on until the entire tree is parsed. The grammar-

representation thus obtained corresponding to this parse-tree for benzene is indicated in the figure's caption.
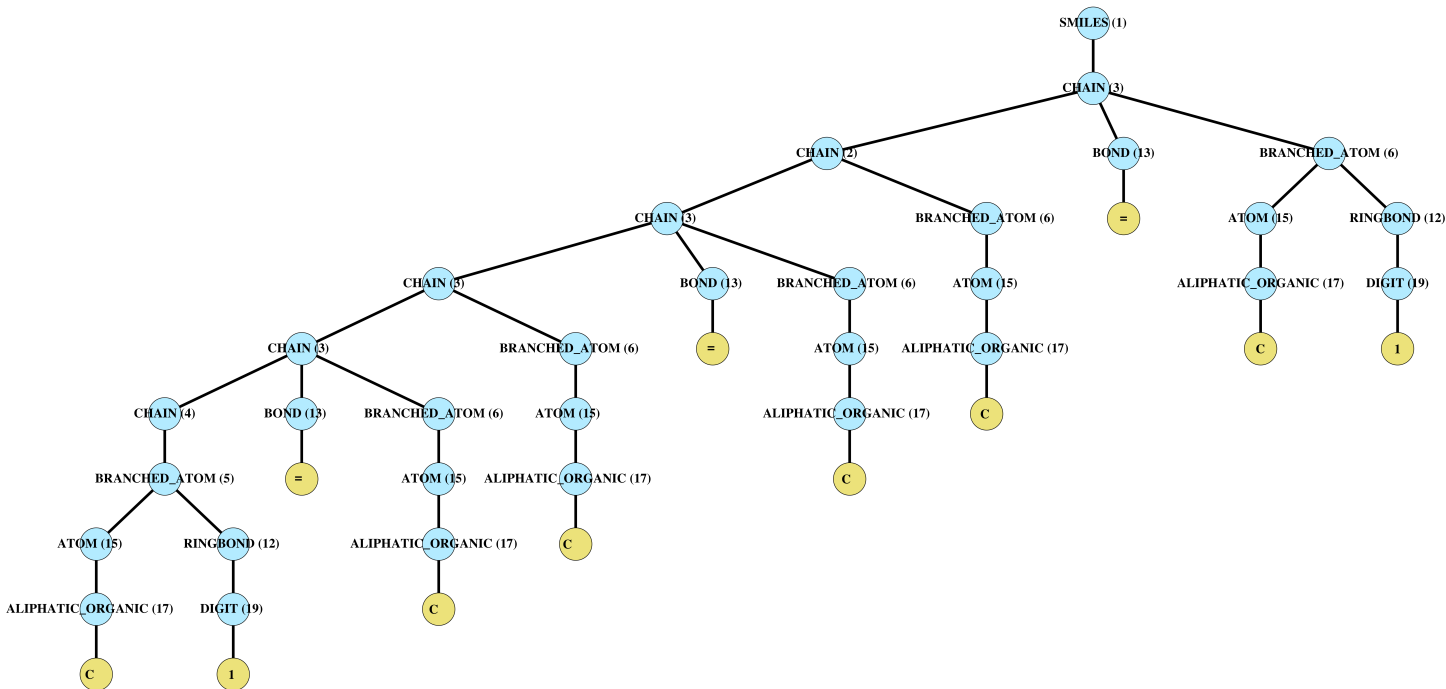

Figure 2: The parse-tree obtained for benzene with SMILES string representation as `C1=CC=CC=C1`. The production rules from Table 1 applied at each stage are indicated next to the non-terminal symbols. Parsing this tree in a bottom-up-left-corner strategy gives rise to the grammar-representation given by: $1, 3, 2, 3, 3, 4, 5, 15, 17, 12, 19, 13, 6, 15, 17, 6, 15, 17, 13, 6, 15, 17, 6, 15, 17, 13, 6, 15, 17, 12, 19$

Clearly, as compared to a purely character-based SMILES string representation consisting merely of the tokens 'C', '1', '=', 'C', 'C', '=', 'C', 'C', '=', 'C', '1', without any additional information conveying the relationships between the tokens, the grammar-based representations are significantly richer, incorporate chemical and structural information, and contain hierarchical information about the underlying chemistry that could be leveraged by the model architecture for modeling the underlying grammar. Such representations are shown to be more efficient in modeling the underlying chemistry and eliminate overparameterization in complex machine learning architectures [24]. We present an information-theoretic analysis of the grammar-representations and the text-based representations in Section 4 to establish the fundamental superiority of the grammar-representations compared to other text-based representations such as SMILES.

7

3.2. Sequence-to-sequence models

We model the reaction prediction problem as a sequence modeling task that involves mapping the input sequence to a sequence of tokens that corresponds to the output sequence. This framework has been used in recent years and has shown a significant promise in reaction modeling. We use the state-of-the-art model in this area, known as the transformer framework, proposed in [26].
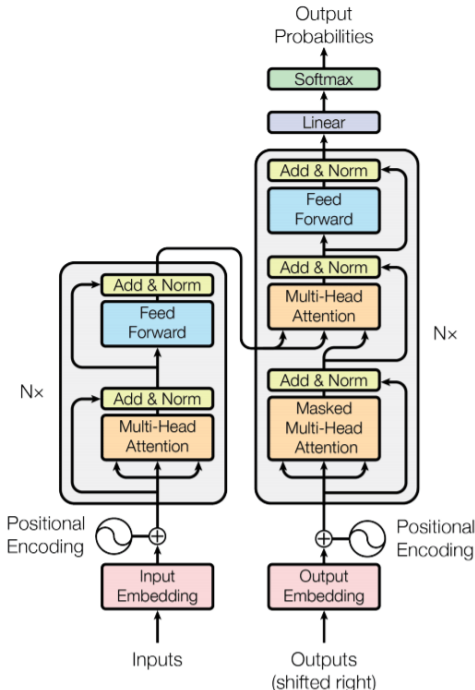

Figure 3: The encoder-decoder model architecture of a transformer

The transformer framework, shown in Figure 3, consists of an encoder-decoder architecture where the encoder maps the input sequence to a latent space, and the decoder decodes from the latent space in an autoregressive manner, one element at a time, to give rise to the output sequence. The positional encodings in a transformer encode the position of a given word (or token) in the sequence to a high dimensional vector space, getting rid of recurrent or convolution operations that significantly improved the computational complexity of training the model architecture. These mappings are characterized by sines and cosines of different frequencies, given by

$$
\vec{p}_{pos,i} = \begin{cases} sin(pos/10000^{2k/d}), & \text{if } i = 2k \\ cos(pos/10000^{2k/d}), & \text{if } i = 2k+1 \end{cases} \tag{1}
$$

An attention-mechanism lets the transformer model relationships between groups of words in an input sequence at different stages of the network. The attention-mechanism used in [26] is the 'Scaled-Dot Product Attention', characterized by a set of queries, keys, and values vectors. The query and key vectors are of dimensions d_k, and the value vector is of dimension d_v. The attention-score then is computed as softmax function applied over the dot-products of the queries and key vectors, scaled down by a factor of $\sqrt{d_k}$, given by

$$Attention(Q, K, V) = softmax(\frac{QK^T}{\sqrt{d_k}})V \tag{2}$$

where Q, K, and V are the matrices of query, key, and values vectors, respectively. The attention score computed above determines the importance of different parts of an input sequence in the current context. In order to allow the model to jointly factor in information from different representation subspaces at different positions, multi-headed attention is computed, which involves computing multiple attention scores in parallel, which are then concatenated and projected using a linear transformation to compute the multi-head attention scores as,

$$MultiHead(Q, K, V) = Concat(head_1, head_2, \ldots, head_h)W^O \tag{3}$$

where $head_i = Attention(QW_i^Q, KW_i^K, VW_i^V)$, and $W_i^Q \in \mathbb{R}^{d_{pos} \times d_k}$, $W_i^K \in \mathbb{R}^{d_{pos} \times d_k}$, and $W_i^V \in \mathbb{R}^{d_{pos} \times d_v}$ are the projection matrices for Q, K, and V, respectively.

3.3. Beam search

In order to get the output sequences in a transformer framework, a decoding procedure is used that decodes from the latent space in an autoregressive manner, with the current prediction as input while decoding the next token. Therefore, the decoding procedure could either employ a greedy strategy that involves selecting the token with the maximum likelihood at each stage for decoding the next token, generating a single most-likely sequence in the end, or on the other hand, it could employ a beam search procedure that decodes a set of top-B tokens at each stage based on their likelihood and give rise to top-B sequences as the output of the model. We follow the latter approach for decoding. This allows us to evaluate our model's performance more extensively and compare it with the top-K accuracy reported in other similar works in this area. A schematic of

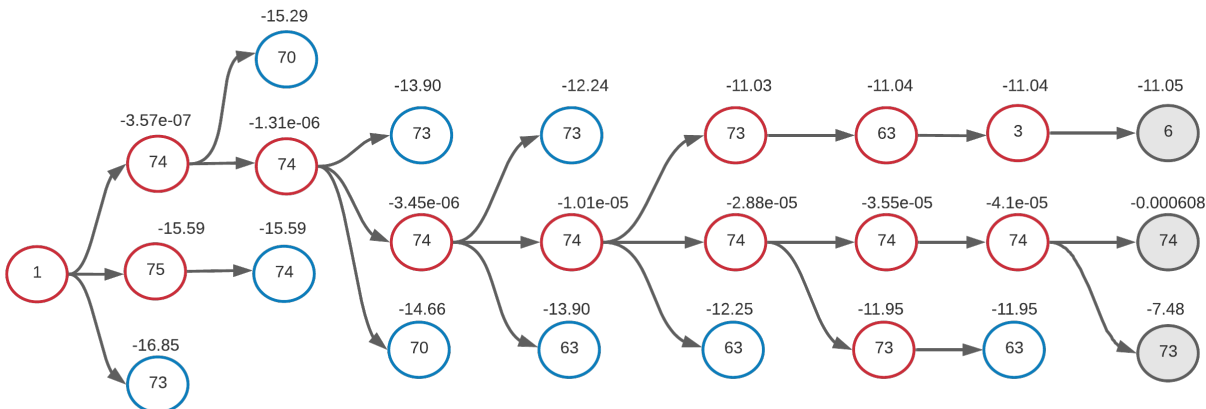the beam-search decoding procedure used in our work is shown in Figure 4.

Figure 4: A partially completed beam search output for a beam width of 3 for a reference input. At each stage, the most likely grammar-rules are predicted in the above schematic that would be used to reconstruct the corresponding SMILES string. The log-likelihood values are indicated above each node in the schematic.

4. Information-Theoretic Analysis of Chemical Representations

Before we discuss the model training aspects, we demonstrate the richness of the proposed grammar-based representations using an information-theoretic framework. We compare the information capacity, information gain, and redundancy characterizing the various symbols-based chemical representations, namely, molecular formula, SMILES, and grammar representations. We first provide a brief overview of the relevant information-theoretic concepts and their intuition in the next section, followed by their application to chemical representations and quantify the superiority of grammar-based representations from an information-theoretic standpoint.

4.1. Shannon Entropy and Information Content

The development and formalization of information theory, mainly by Claude Shannon in [29], offered a mathematical definition of the *amount of information* communicated between any two components or channels of a given system. The primary motivation was the fundamental problem of decoding a source message passing through a noisy channel, either exactly or approximately, at any other point in the communication system. However, the applications and adaptations of it are not limited to communication systems alone but have had far-reaching consequences across most fields of science and engineering.

10

The Shannon entropy for a given probability distribution $p(x)$ of a random variable x is defined as,

$$H = -\sum_{i=1}^{M} p(x_i) \log_2 p(x_i) \tag{4}$$

where $p(x)$ is the probability mass function of x with M possible values. This is equivalent to the expected value of the Shannon information or self-information of a variable and is measured in units of *bits per symbol*. There is a direct correspondence between the amount of information in a message and the degree of uncertainty that is associated with it. That is, if a system can exist in one of a very large number of possible states, then there is a great amount of uncertainty associated with its state as opposed to another system that can exist only in a handful states. Therefore, the amount of information required is more for the former than the latter.

Consider the two extremes of zero-information content and maximum information content. The Shannon entropy in Equation 4 attains a value of zero when the probability $p(x_i)$ of a x_i attaining a given value is 1 meaning that the outcome or the value that x_i could take is known with complete certainty, and hence, there is no information content (or gain) associated with knowing its value explicitly. On the other hand, when x_i could take any of the possible values with equal probability, i.e., $p(x_i) = 1/M$ where M is the total number of possible values that the symbols in the source message could take, the information content is maximized and is equal to $\log_2 M$. This implies that in such a scenario, specifying the value of a given bit in the sequence would result in the maximum information gain when compared to any other scenario.

The generalization of Equation 4 when several random variables $X_1, X_2, \ldots, X_n$ are present is given by the joint Shannon entropy as,

$$H(X_1, X_2, \ldots, X_n) = -\sum_{x_1, x_2, \ldots, x_n} p(x_1, x_2, \ldots, x_n) \log_2 p(x_1, x_2, \ldots, x_n) \tag{5}$$

The joint entropy in Equation 5 could be interpreted as an information measure corresponding to multiple random variables presented simultaneously. Similarly, the conditional entropy that quantifies the information content of a given random variable X_1 conditioned on a set of other

11

random variable $X_2, X_3, \ldots, X_n$, is given as

$$H(X_1 \mid X_2, X_3, \ldots, X_n) = - \sum_{x_1, x_2, \ldots, x_n} p(x_1, x_2, x_3, \ldots, x_n) \log_2 p(x_1 \mid x_2, x_3, \ldots, x_n) \qquad (6)$$

The conditional entropy could be used to measure the information gain when partial information or context of other random variables is known.

Equipped with information theory concepts, we now apply these information measures to chemical systems and molecules.

4.2. Information theory and Chemical Representations

Studies in chemical information theory [30] have demonstrated the promise of entropic perspective in chemistry [31, 32, 33, 34]. We analyze various chemical representations, namely, the SMILES representations, molecular formulas, and our proposed SMILES grammar-based representations from the perspective of Shannon entropy. We quantify the superiority of certain representations when compared to the others and highlight their inherent benefits when used in machine learning algorithms.

In our framework, we consider the individual tokens in various representations as random variables that contain *bits of information* required to reconstruct a given molecule. The representations are therefore a sequence of random variables, $X_1, X_2, \ldots, X_n$, where n is the length of the representation for a given molecule and X_i could take any of the M possible tokens defined in the vocabulary of the representation. For instance, consider the earlier example of benzene from Section 3.1. The corresponding random variables for each of the three representations is given by,

- Molecular formula (C_6H_6): $X_i^{Mo} \in \{\text{'}C\text{'}, \text{'}6\text{'}, \text{'}H\text{'}\}$, where $M = 3, n = 4$

- SMILES ($C1 = CC = CC = C1$): $X_i^{S} \in \{\text{'}C\text{'}, \text{'}1\text{'}, \text{'} = \text{'}\}$, where $M = 3, n = 4$

- Grammar[1]$(1, 3, 2, 3, \ldots, 12, 19)$: $X_i^{G} \in \{1, 2, 3, 4, 5, 6, 12, 13, 15, 17, 19\}$, where $M = 11, n = 32$

Defining the random variables and computing their probability distributions over all the molecules in the dataset, we could compute the corresponding information measures using Shannon entropy

---

[1]using the representative grammar in 1

in Equation 4. Since our objective is to quantify the information capacity for an entire representation instead of certain specific molecules, this distribution is computed over all the possible lengths of representations, n, in the dataset. Similarly, the conditional information measure in Equation 6 could be computed using the conditional distribution of random variables, computed using the co-occurrence matrices (up to a given order) of the random variables in the database. The order indicates the number of random variables under consideration, with $\eta - 1$ conditioned random variables for an order of η. An order $\eta = 1$ corresponds to Shannon entropy (Equation 4), order $\eta = 0$ corresponds to Shannon entropy when the random variables follow a uniform distribution, and orders $\eta > 1$ correspond to conditional entropy with conditioning on $\eta - 1$ random variables.

The probability distributions for the random variables are computed using the three representations for all the molecules in the test-set of the USPTO 50K reaction dataset to limit computational requirements, especially for calculating the conditional distributions. We evaluate the maximum conditional distribution up to an order of $\eta = 5$. The molecular formulas are extracted from the SMILES representation of a given molecule using the 'rcdk' library in R. The conditional information measure at different values of the order is presented in Figure 5 and Table 2.
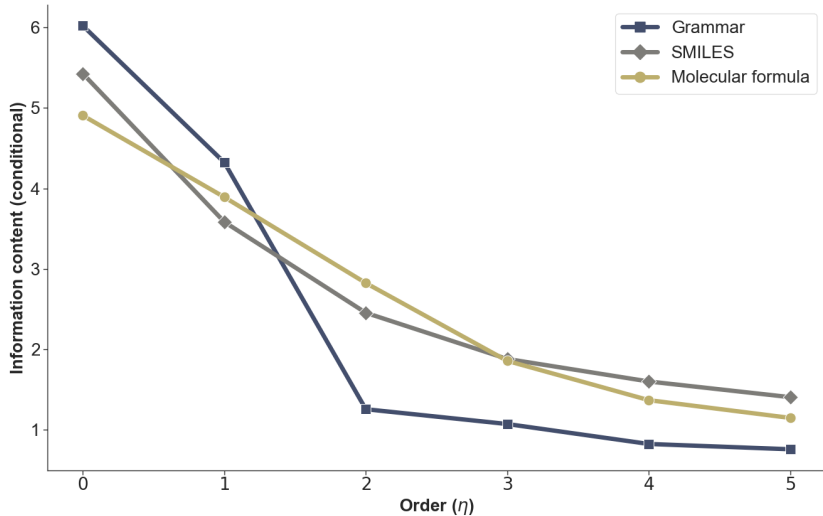

Figure 5: Information content vs order of conditioning (η) for the three representations

Table 2: Information content (i_η) for various orders of conditioning (η) for the three representations

	Molecular Formula	Grammar	SMILES
i_0	5.426	6.022	4.906
i_1	3.583	4.322	3.891
i_2	2.453	1.254	2.823
i_3	1.879	1.070	1.855
i_4	1.599	0.822	1.367
i_5	1.404	0.756	1.146

It follows from our discussion in the earlier section that the maximum information (corresponding to i_0) is achieved when the random variables follow a uniform distribution and all the bits have the same probability ($1/M$) of taking a given value. Thus, i_0 is independent of the dataset under consideration and is purely a property of the representation that is indicative of its information storing capacity. Based on Figure 5, the grammar-representations have much higher information capacity, followed by the SMILES representation and then the molecular formulas, highlighting the theoretically high information capacity of grammar representations.

When the order of analysis is increased to 1, the information capacity decreases for all the representations, indicating that the underlying probability distributions are far from uniform, with certain values more likely than others. This is expected since in any chemical representation, the identifiers for atoms such as C and H are significantly more likely to occur when compared to others such as F or B. It could be inferred through the probability versus identifier index plot depicted in Figure 6 that the SMILES and molecular formula representations are much more skewed, with a majority of the identifiers occurring much more frequently than the others. On the other hand, the grammar-based representations' identifiers exhibit a much smoother and slower decay, indicating more evenly distributed probabilities for the identifiers. This validates the richness of grammar-representations due to the incorporation of structural-hierarchy, an argument that we made qualitatively in our earlier work [24].
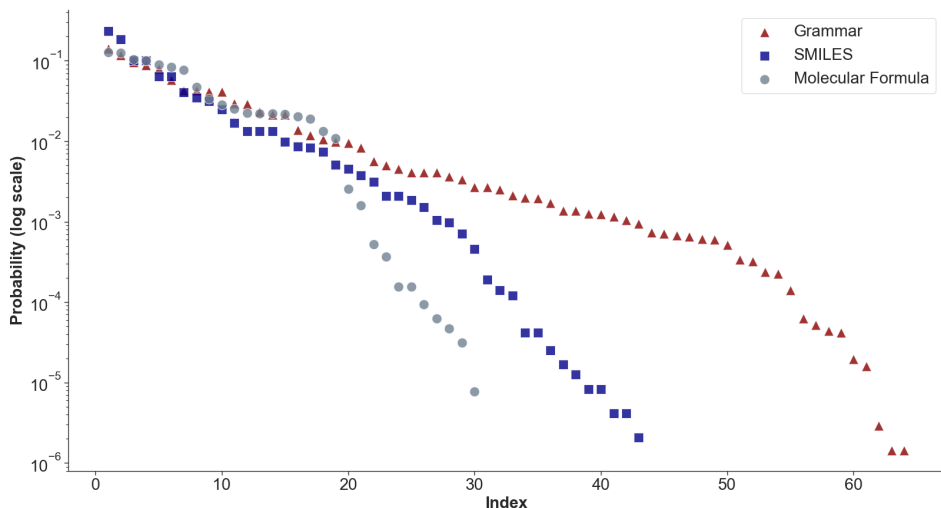
Figure 6: Probability of occurrence of a given token versus the sorted index

As the order of conditioning while computing the information measure is increased to $\eta = 2$, a drastic decrease in the information content is observed for grammar-representations, and the conditional information content remains significantly lesser than the other representations even for higher values of η. This could be attributed to the in-built redundancy in the grammar-representations incorporated by means of a hierarchical sequence of production rules encoded in a molecule's representation. This transforms into lower values of conditional probabilities when an identifier's context in terms of the preceding tokens is known. Qualitatively, this means that when the context of a token is provided, the uncertainty associated with the possible values it could take is much lesser than its equivalent in the SMILES representation and molecular formula-based representations, as seen in Figure 5.

In summary, the underlying redundancy in grammar-representations, indicated by i_η with $\eta \geq 2$, could be leveraged by machine learning algorithms that model the long and short-range dependencies between tokens in a given sequence, such as the class of sequence-to-sequence models used in our work. In addition, the higher information-storage capacity of these representations, as indicated by i_0 and i_1, implies that they are much richer when compared to the other representations and therefore contain additional *bits of information* that is lacking in the other representations and could be crucial for the adequate differentiation between molecules in the latent space.

15

5. Data and Model training

We demonstrate our model's performance using a standard retrosynthesis prediction dataset which is a filtered dataset derived from the text extraction work done on US Patents and Trademark Office's (USPTO) database [35] and further classified into ten different reaction classes [36]. The filtered dataset contains only the reactants and products, with the reagent information removed and the SMILES strings canonicalized. Further, similar to [16], the multiple product reactions are split into multiple reactions so that each reaction contains only a single major product. This dataset is referred to as the USPTO 50K dataset in the literature.

In order to use our approach, we encode the SMILES strings corresponding to all the molecules in the database to their equivalent grammar representations as described in Section 3.1. This implies that since we are working with a subset of the official OpenSMILES grammar, certain molecules that are not in grammar are skipped and therefore are not included in the model training stage. Table 3 summarizes the reaction database with the number of reactions that are in grammar along with the train, validation, and test-set splits. Table 4 summarizes the distribution of the various reactions across the 10 reaction classes.

Table 3: An overview of the retrosynthesis dataset used in our work

Dataset	train	valid	test	total
USPTO 50K				
with (sanitized) molecules	40,029	5,004	5,004	50,037
in grammar	38,995	4,861	4,861	48,717

Table 4: Distribution of reactions across different reaction classes that are in-grammar

Reaction class	Reaction name	train	valid	test	**total**
1	Heteroatom alkylation and arylation	11,886	1,476	1,478	14,840
2	Acylation and related processes	9,358	1,165	1,169	11,698
3	C – C bond formation	4,324	544	539	5,407
4	Heterocycle formation	710	89	90	889

Table 4: Distribution of reactions across different reaction classes that are in-grammar

Reaction class	Reaction name	train	valid	test	**total**
5	Protections	513	64	62	639
6	Deprotections	6,357	796	789	7,942
7	Reductions	3,607	448	452	4,507
8	Oxidations	629	80	79	788
9	Functional group interconversion (FGI)	1,434	176	180	1,790
10	Functional group addition (FGA)	177	23	23	223

Since the retrosynthesis prediction task involves predicting a set of precursors that could be used for obtaining a given product molecule, we define identifiers that distinguish the various reactant molecules (grammar-representation) from each other and also indicate the end of the set. These two additional tokens convey to the model the separation between various precursors' representations and also the end of the entire set of precursors. The reaction class identifiers are appended at the start of the source (product) molecule's representation. A schematic for this is shown in Figure 7.
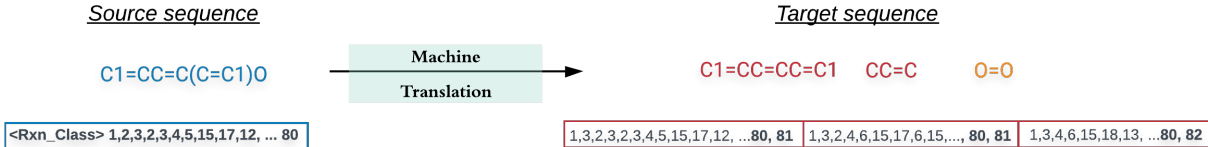

Figure 7: The retrosynthesis reaction encoding strategy used in the machine translation framework. The identifier '80' indicates the end of a given molecule's grammar-representation, '81' indicates the separation between two precursor molecules, and '82' indicates the end of the entire set of precursor molecules.

We train the transformer model for this task using a cross-entropy-based loss function that minimizes the sequence-to-sequence translation error. The model was trained using the Adam optimizer [37] with beta $\beta_1 = 0.9$, $\beta_2 = 0.98$, and $\epsilon = 10^{-9}$, and a cyclic learning rate schedule that is characterized by a fixed number of warmup steps given by

$$lr = d_{model}^{-0.5}.min(step\_num^{-0.5}, step\_num * warmup\_steps^{-0.5}) \tag{7}$$

where d_model is the embedding dimension (positional). At the training stage, to avoid overfitting, a dropout layer is used for both the feed-forward networks and the attention-mechanism, for the encoder and the decoder. A masking approach similar to [38] is used for generating the output SMILES strings from the decoded grammar-representation. A loss function based on sparse categorical cross-entropy between the predicted and actual target sequences is minimized. The possible and the best hyperparameters identified for the model are given in Table 5. The lengths of the input and output representations to the model are fixed at 301 and 900, respectively.

The model was trained using TensorFlow 2.1 and python 3.7 for 12 cycles ($\sim$700 epochs). For generating the parse-trees and extracting grammar-based features, we use the Natural Language ToolKit (NLTK) 3.4.5 library. The molecular datasets were processed using the 2019 release of the RDKit library.

Table 5: Possible and best hyperparameter values for the transformer model architecture described in Figure 3

Hyperparameter	Possible values	Final model
Embedding dimensions	64, 128, 256	256
Attention heads	4, 8, 16	8
Feedforward network units	512, 1024, 2048	512
Number of layers	4, 6	4
Dropout	0.1, 0.2	0.1
Warmup steps	4k, 8k, 12k	8k

6. Results and Discussion

In this section, we define the performance metrics, evaluate the model's performance on the test-set of the USPTO 50K dataset, and benchmark the performance of our approach against other similar works in this area, highlight the advantages and limitations of this framework.

6.1. Evaluation metrics

We evaluate our model's performance using the following metrics – accuracy, which captures the accuracy of perfectly predicting all the precursor molecules; fractional accuracy, which indicates

the fraction of accurately predicted precursors from the ground truth; and syntactic validity, meaning the percentage of grammatically valid predictions. In addition, we also compute the accuracy of prediction of the Maximal Fragment or MaxFrag [22] indicating the prediction accuracy of the longest reactant involved and report the average BLEU (bilingual evaluation understudy) [39] and similarity scores for the maximal fragment molecule. The BLEU score is a standard metric used for evaluation of the quality of machine-translated texts against a reference translation, and the similarity scores[2] are computed using the similarities between the string substructures of the predicted and the true MaxFrag molecules. These metrics are reported for three example predictions in Figure 8.

6.2. Results on USPTO 50K dataset

The performance evaluation measures computed on the test set of the USPTO 50K dataset are presented in Tables 6 and 7. We observe from Table 6 that though the top-10 accuracy is 66.6%, the fractional accuracy at 73.7% is much higher and indicates that a major fraction of the ground truth reactants is accurately predicted across reactions. The syntactic validity is as high as 95.6% for the top-1 predictions and 90.4% for the top-10 predictions. The decreasing trend in syntactic validity is expected since as the number of predictions increases, the invalid predictions go up because of the model's susceptibility to decode grammatically invalid strings.

Performance measure	top-1	top-3	top-5	top-10
Accuracy	43.8	57.2	61.4	66.6
Fractional accuracy	53.8	65.4	69.2	73.7
Syntactic validity	95.6	92.8	91.6	90.4

Table 6: Accuracy, fractional accuracy, and syntactic validity of the model results on the test set

The similarity scores in Table 7 indicate that the MaxFrag precursor is predicted with a top-10 accuracy of over 70% and a similarity score of over 90%, highlighting the model's ability to
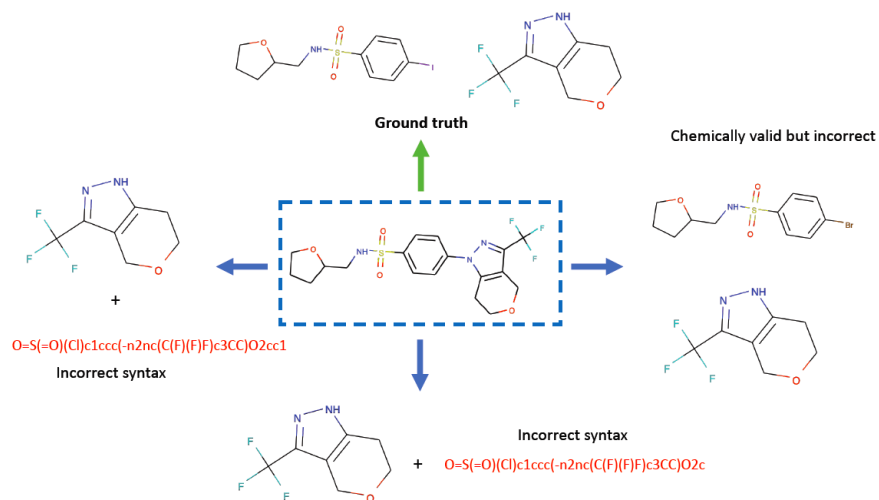
---

[2]computed using the SequenceMatcher routine in python that matches the longest contiguous matching subsequence that does not contain any unwanted (or junk) elements

correctly identify the characteristics of the most critical molecule (in classical retrosynthesis) with a fairly high degree of accuracy. The corresponding BLEU scores also indicate the good quality of translation that is achieved for the MaxFrag molecule.
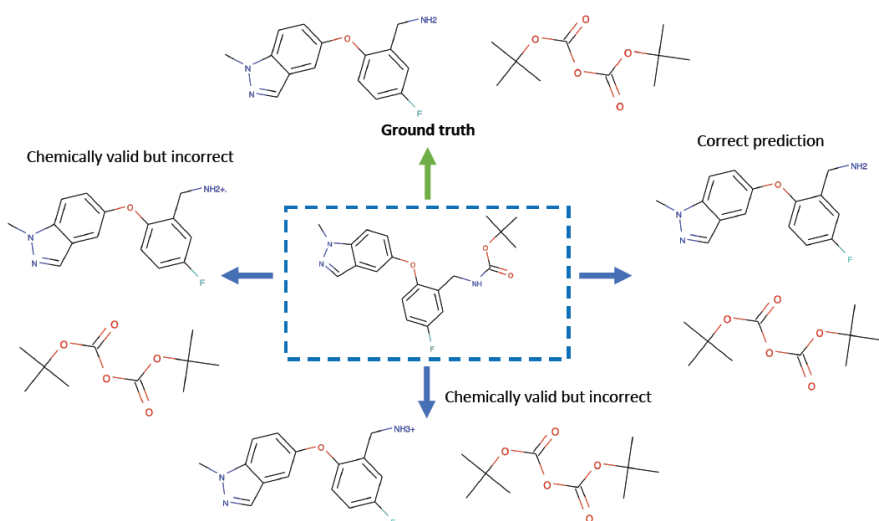
Performance measure	top-1	top-3	top-5	top-10
MaxFrag accuracy	50.4	62.1	65.7	70.2
BLEU score	74.8	83.4	85.2	87.4
Similarity score	80.0	87.2	88.6	90.2

Table 7: MaxFrag accuracy and the corresponding BLEU and similarity scores on the test set
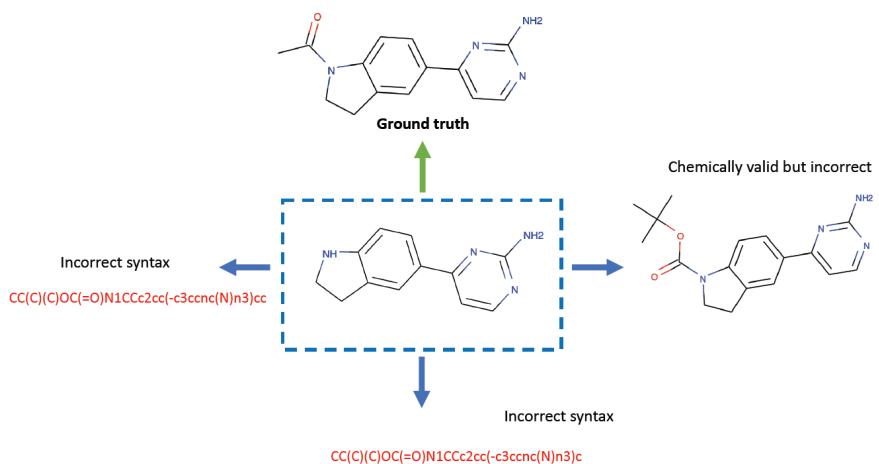
Some of the example top-3 predictions along with the prediction inaccuracies and performance metrics are presented in Figure 8.

(a) Example from reaction class 1; accuracy: 0.0, fractional accuracy: 0.5; syntactic validity: 0.67, MaxFrag accuracy: 0.0, MaxFrag similarity: 0.56 , MaxFrag BLEU: 0.36

(b) Example from reaction class 5; accuracy: 1.0, fractional accuracy: 1.0; syntactic validity: 1.0, MaxFrag accuracy: 1.0, MaxFrag similarity: 1.0 , MaxFrag BLEU: 1.0

(c) Example from reaction class 6; accuracy: 0.0, fractional accuracy: 0.0; syntactic validity: 0.33, MaxFrag accuracy: 0.0, MaxFrag similarity: 0.89 , MaxFrag BLEU: 0.79

Figure 8: Example top-3 predictions made by our model and their corresponding evaluation metrics indicated in the figure captions

21

6.3. Performance across reaction classes

In order to further understand the performance of our model across reaction classes, we increase the granularity of the analysis and compute the five metrics– accuracy, fractional accuracy, MaxFrag accuracy, similarity score, and syntactic validity across the 10 reaction classes. The detailed measures of these metrics are summarized in Tables 8, 9, 10, and 11. The fraction of invalid predictions across the various reaction types for top-10 analysis are presented in Figure 9.
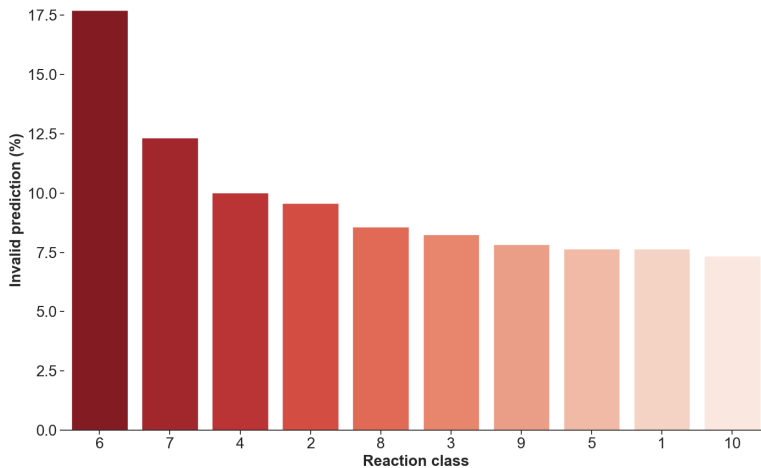

Figure 9: Invalid SMILES strings percentages on top-10 predictions

The above trend indicates that except for reaction class 6 (deprotections), all the reaction types give rise to the same percentage of invalid predictions. A likely possibility for this observation could be the model learning the underlying grammar, irrespective of the number of samples in each class or the chemical transformations occurring across the different reaction types. This behavior is not trivial since the corresponding top-10 prediction accuracy in Table 11 does not follow the same trend across reaction classes. The high percentage error in deprotection reactions could be attributed to several factors that could be specific to the reaction class and could be analyzed through chemistry-driven heuristics that we envision as a hybrid explanation-generation system as a future extension of this work.

Top-1 measure	Reaction class									
	1	2	3	4	5	6	7	8	9	10
Accuracy	40.9	52.2	37.7	26.7	66.1	35.4	50.4	69.6	38.3	56.5
Fractional accuracy	54.9	67.0	49.9	39.4	81.5	35.4	50.4	75.3	45.0	71.7
Syntactic validity	96.7	95.8	96.4	94.1	97.6	90.9	95.2	97.1	98.8	97.8
MaxFrag accuracy	50.3	61.3	44.9	37.8	83.9	35.4	50.4	77.2	44.4	60.9
MaxFrag similarity	82.0	86.2	78.6	71.2	91.8	68.0	79.5	89.0	78.4	82.9

Table 8: The top-1 accuracy, fractional accuracy, MaxFrag accuracy and MaxFrag similarity scores across the reaction classes (in %)

Top-3 measure	Reaction class									
	1	2	3	4	5	6	7	8	9	10
Accuracy	54.3	66.6	51.4	31.1	80.6	49.9	61.3	77.2	51.7	73.9
Fractional accuracy	66.3	77.4	62.5	49.4	89.5	49.9	61.3	82.9	57.8	80.4
Syntactic validity	94.5	92.6	93.9	91.8	94.4	86.3	89.6	94.4	95.6	91.9
MaxFrag accuracy	61.0	72.1	58.3	46.7	90.3	49.9	61.3	84.8	58.9	73.9
MaxFrag similarity	87.0	91.5	84.3	80.3	98.4	81.0	89.2	96.0	88.0	89.4

Table 9: The top-3 accuracy, fractional accuracy, MaxFrag accuracy and MaxFrag similarity scores across the reaction classes (in %)

Top-5 measure	Reaction class									
	1	2	3	4	5	6	7	8	9	10
Accuracy	59.3	70.9	54.5	36.7	83.9	53.9	64.4	79.7	56.7	73.9
Fractional accuracy	70.7	80.9	66.0	53.9	91.1	53.9	64.4	84.8	61.7	80.4
Syntactic validity	93.4	91.6	92.6	90.9	92.6	84.0	88.9	93.2	94.3	91.6

Top-5 measure	Reaction class									
	1	2	3	4	5	6	7	8	9	10
MaxFrag accuracy	65.2	75.7	61.0	50.0	93.5	53.9	64.4	87.3	62.2	73.9
MaxFrag similarity	88.5	92.2	85.6	81.2	98.5	83.3	90.3	99.2	88.2	89.2

Table 10: The top-5 accuracy, fractional accuracy, MaxFrag accuracy and MaxFrag similarity scores across the reaction classes (in %)

Top-10 measure	Reaction class									
	1	2	3	4	5	6	7	8	9	10
Accuracy	65.1	75.4	60.3	41.1	85.5	58.6	70.6	82.3	63.3	78.3
Fractional accuracy	75.5	84.2	70.5	58.3	91.9	58.6	70.6	86.7	67.8	82.6
Syntactic validity	92.3	90.4	91.8	90.0	92.3	82.3	87.7	91.4	92.2	92.7
MaxFrag accuracy	69.8	79.4	65.7	53.3	93.5	58.6	70.6	88.6	67.8	78.3
MaxFrag similarity	90.1	93.5	87.8	82.9	98.6	85.0	92.0	98.9	90.5	91.8

Table 11: The top-10 accuracy, fractional accuracy, MaxFrag accuracy and MaxFrag similarity scores across the reaction classes (in %)

6.4. Comparison with other work

Here, we compare the performance of our model against other similar work in this area. One of the first benchmarks in retrosynthesis prediction using seq2seq models on SMILES string representations is by Liu et al. [16]. Their framework is similar to ours in that there are no post-processing of predictions, data augmentation strategies, and model performance-boosting methods used for further improving the model performance – techniques that usually result in improved accuracy custom-fit to a given setting. Our objective is to propose an alternative formulation that is fundamentally different from the other approaches in that it ensures incorporation of chemistry knowledge, forcing the model parameters to learn the underlying grammar-representations to minimize invalid predictions.

24

Table 12 compares the prediction accuracies against those reported in Liu et al. We observe that our model improves the prediction accuracy by a margin of $\sim 5\%$ across all the top-N measures and reduces the percentage of invalid predictions by $53\% - 64\%$. We attribute the higher accuracy and the decrease in invalid predictions to the grammar-representations that incorporate structural information about the molecules and are characterized by much higher redundancies when compared to SMILES strings as demonstrated using the information-theoretic framework in Section 4.

Table 12: Comparison with other similar works involving purely seq2seq models and USPTO 50K dataset

Model	Top-N measure accuracy (%) | invalid (%)			
	1	3	5	10
Liu Seq2Seq [16]	37.4 | 12.2	52.4 | 15.3	57.0 | 18.4	61.7 | 22.0
Our work	43.8 | 4.4	57.2 | 7.2	61.4 | 8.4	66.6 | 9.6

Figure 10 demonstrates our model's ability to outperform the top-10 accuracy reported in Liu et al. across reaction classes, often by a significant margin.
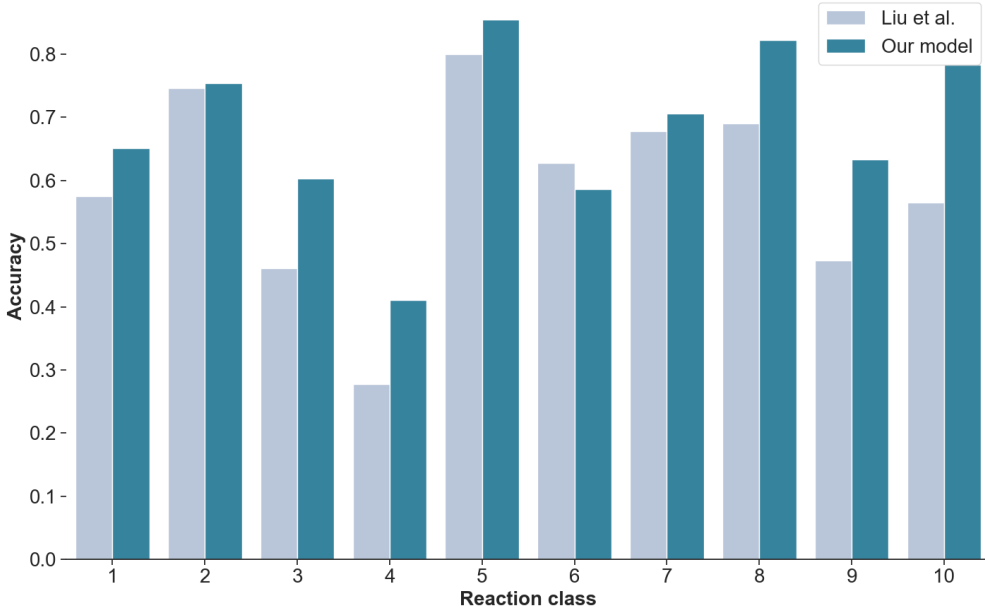

Figure 10: Comparison of top-10 accuracies across reaction classes

As mentioned earlier, it is possible to achieve higher prediction accuracy through additional performance boosting techniques as demonstrated in the following studies. Zheng et al. [40] used an additional transformer model that takes as input the output of another transformer model to correct the invalid predictions. Tetko et al [22] proposed data augmentation strategies that significantly increase the size of the dataset used for building a transformer model for retrosynthesis. Karpov et al. [19] used model ensembling, snapshot learning methods, and increasing beam search temperature to improve the model performance. Lin et al. [17] used averaging of model weights and combination with Monte Carlo search tree strategies for proposing retrosynthesis routes. We believe that combining our approach with the techniques mentioned above for improving the model performance would boost our model's accuracy as well, but at the cost of significantly higher computational requirements.

7. Conclusions

Retrosynthesis analysis is a challenging problem since it involves predicting the precursors for the synthesis of a given molecule with limited information, a much higher number of possible synthesis pathways as compared to the forward reaction prediction problem, and approximation of an often complex multi-step analysis as a single-step prediction problem. Naturally, incorporating additional information about the reaction or the molecules involved would be of immense use given the complexity of the task and the limited information often present for making the predictions. Towards that goal, we have proposed grammar-based representations of molecules that incorporate chemical and structural information extracted from their SMILES string representations.

Such representations are shown to be successful in overcoming over-parameterization in models for the forward reaction prediction in our earlier work [24]. Here, we have quantified the superiority of such representations from an information-theoretic standpoint. We have shown that these representations have theoretically higher information capacity, which is validated through the Shannon entropy computed on reactions in the USPTO 50K dataset. Moreover, the conditional entropy measures calculated at higher orders highlight the significantly higher redundancy in-built in these representations that make them suitable for machine learning architectures, especially the seq2seq class of models that are used for such tasks.

The performance of our model reinforced the above observations. We report the top-1 prediction

accuracy of 43.8% and syntactic validity of 95.6% as opposed to 37.4% and 87.8%, respectively, reported in Liu et al. We have shown that not only does our model outperform the aggregate statistics reported in Liu et al., the performance of our model across the various reaction classes is much better. An interesting observation is that owing to the grammar-representations, our model results in nearly the same percentage of invalid predictions across reaction classes – independent of reaction type and the number of reactions in training set in each category. Moreover, the analysis of the MaxFrag accuracy and the corresponding similarity and BLEU scores indicate the accurate prediction of the major precursor involved in the synthesis of a given molecule.

In summary, we have proposed a novel formulation of the retrosynthesis reaction prediction problem that incorporates rich, hierarchical, molecular structure information and is superior from an information-theoretic standpoint. This formulation significantly outperforms the other model in this class of seq2seq models that uses SMILES representations of molecules – both in terms of higher prediction accuracy and lesser grammatically invalid predictions. The future extension of our work would involve solving the multi-step retrosynthesis problem and incorporating additional contextual information about the reactions into the same framework.

Acknowledgements

Appendix

The SMILES grammar used in this work is the same as that used in our previous work on the forward prediction problem [24]. This grammar comprises 80 production rules with 24 non-terminals symbols specifying the different structural components of a SMILES string. All the production rules for the grammar used in our work are summarized in Table 13. The first and the last production rules, SMILES ⟶ CHAIN and NOTHING ⟶ NONE, are additional rules included signifying the start and end of a SMILES string, which is analogous to the <START> and <END> tokens in natural language processing marking the beginning and the end of sentences, respectively.

Table 13: SMILES grammar used in GO-PRO [24]

S.No	Production rules
1	SMILES ⟶ CHAIN
2	ATOM ⟶ BRACKET_ATOM | ALIPHATIC_ORGANIC | AROMATIC_ORGANIC
3	ALIPHATIC_ORGANIC ⟶ B | C | N | O | S | P | F | I | Cl | Br
4	AROMATIC_ORGANIC ⟶ c | n | o | s | p
5	BRACKET_ATOM ⟶ [BAI]
6	BAI ⟶ ISOTOPE SYMBOL BAC | SYMBOL BAC | ISOTOPE SYMBOL | SYMBOL
7	BAC ⟶ CHIRAL BAH | BAH | CHIRAL
8	BAH ⟶ HCOUNT BACH | BACH | HCOUNT
9	BACH ⟶ CHARGECLASS | CHARGE | CLASS
10	SYMBOL ⟶ ALIPHATIC_ORGANIC | AROMATIC_ORGANIC | ELEMENT_SYMBOLS
11	ISOTOPE ⟶ DIGIT | DIGIT DIGIT | DIGIT DIGIT DIGIT
12	DIGIT ⟶ 1 | 2 | 3 | 4 | 5 | 6 | 7 | 8
13	CHIRAL ⟶ @ | @@
14	HCOUNT ⟶ H | H DIGIT
15	CHARGE ⟶ - | - DIGIT | - DIGIT DIGIT | + | + DIGIT | + DIGIT DIGIT
16	BOND ⟶ - | = | # | / | \\
17	RINGBOND ⟶ DIGIT | BOND DIGIT
18	BRANCHED_ATOM ⟶ ATOM | ATOM RB | ATOM RB BB
19	RB ⟶ RB RINGBOND | RINGBOND
20	BB ⟶ BB BRANCH | BRANCH
21	BRANCH ⟶ (CHAIN) | (BOND CHAIN)
22	CHAIN ⟶ BRANCHED_ATOM | CHAIN BRANCHED_ATOM | CHAIN BOND BRANCHED_ATOM
23	CLASS ⟶ DIGIT
24	ELEMENT_SYMBOLS ⟶ H
25	NOTHING ⟶ NONE

References

[1] David A Pensak and Elias James Corey. Lhasa—logic and heuristics applied to synthetic analysis. ACS Publications.

[2] Timothy D Salatin and William L Jorgensen. Computer-assisted mechanistic evaluation of organic reactions. 1. overview. *The Journal of Organic Chemistry*, 45(11):2043–2051, 1980.

[3] EJ Corey, Alan K Long, Theodora W Greene, and John W Miller. Computer-assisted synthetic analysis. selection of protective groups for multistep organic syntheses. *The Journal of Organic Chemistry*, 50(11):1920–1927, 1985.

[4] William L Jorgensen, Ellen R Laird, Alan J Gushurst, Jan M Fleischer, Scott A Gothe, Harold E Helson, Genevieve D Paderes, and Shenna Sinclair. Cameo: a program for the logical prediction of the products of organic reactions. *Pure and Applied Chemistry*, 62(10):1921–1932, 1990.

[5] Hiroko Satoh and Kimito Funatsu. Sophia, a knowledge base-guided reaction prediction system-utilization of a knowledge base derived from a reaction database. *Journal of chemical information and computer sciences*, 35(1):34–44, 1995.

[6] Koji Satoh and Kimito Funatsu. A novel approach to retrosynthetic analysis using knowledge bases derived from reaction databases. *Journal of chemical information and computer sciences*, 39(2):316–325, 1999.

[7] Jonathan H Chen and Pierre Baldi. No electron left behind: a rule-based expert system to predict chemical reactions and reaction mechanisms. *Journal of chemical information and modeling*, 49(9):2034–2043, 2009.

[8] James Law, Zsolt Zsoldos, Aniko Simon, Darryl Reid, Yang Liu, Sing Yoong Khew, A Peter Johnson, Sarah Major, Robert A Wade, and Howard Y Ando. Route designer: a retrosynthetic analysis tool utilizing automated retrosynthetic rule generation. *Journal of chemical information and modeling*, 49(3):593–602, 2009.

[9] Chris M Gothard, Siowling Soh, Nosheen A Gothard, Bartlomiej Kowalczyk, Yanhu Wei, Bilge Baytekin, and Bartosz A Grzybowski. Rewiring chemistry: Algorithmic discovery and experimental validation of one-pot reactions in the network of organic chemistry. *Angewandte Chemie International Edition*, 51(32):7922–7927, 2012.

[10] Sara Szymkuć, Ewa P Gajewska, Tomasz Klucznik, Karol Molga, Piotr Dittwald, Michał Startek, Michał Bajczyk, and Bartosz A Grzybowski. Computer-assisted synthetic planning: The end of the beginning. *Angewandte Chemie International Edition*, 55(20):5904–5937, 2016.

[11] Marwin HS Segler and Mark P Waller. Modelling chemical reasoning to predict and invent reactions. *Chemistry–A European Journal*, 23(25):6118–6128, 2017.

[12] Marwin HS Segler and Mark P Waller. Neural-symbolic machine learning for retrosynthesis and reaction prediction. *Chemistry–A European Journal*, 23(25):5966–5971, 2017.

[13] Jennifer N Wei, David Duvenaud, and Alán Aspuru-Guzik. Neural networks for the prediction of organic chemistry reactions. *ACS central science*, 2(10):725–732, 2016.

[14] Connor W Coley, Regina Barzilay, Tommi S Jaakkola, William H Green, and Klavs F Jensen. Prediction of organic reaction outcomes using machine learning. *ACS central science*, 3(5):434–443, 2017.

[15] Juno Nam and Jurae Kim. Linking the neural machine translation and the prediction of organic chemistry reactions. *arXiv preprint arXiv:1612.09529*, 2016.

[16] Bowen Liu, Bharath Ramsundar, Prasad Kawthekar, Jade Shi, Joseph Gomes, Quang Luu Nguyen, Stephen Ho, Jack Sloane, Paul Wender, and Vijay Pande. Retrosynthetic reaction prediction using neural sequence-to-sequence models. *ACS Central Science*, 3(10):1103–1113, 2017. PMID: 29104927.

[17] Kangjie Lin, Youjun Xu, Jianfeng Pei, and Luhua Lai. Automatic retrosynthetic route planning using template-free models. *Chemical Science*, 11(12):3355–3364, 2020.

[18] Shuangjia Zheng, Jiahua Rao, Zhongyue Zhang, Jun Xu, and Yuedong Yang. Predicting retrosynthetic reactions using self-corrected transformer neural networks. *Journal of Chemical Information and Modeling*, 60(1):47–55, 2019.

[19] Pavel Karpov, Guillaume Godin, and Igor V Tetko. A transformer model for retrosynthesis. In *International Conference on Artificial Neural Networks*, pages 817–830. Springer, 2019.

[20] Hongliang Duan, Ling Wang, Chengyun Zhang, Lin Guo, and Jianjun Li. Retrosynthesis with attention-based nmt model and chemical analysis of "wrong" predictions. *RSC Advances*, 10(3):1371–1378, 2020.

[21] Philippe Schwaller, Riccardo Petraglia, Valerio Zullo, Vishnu H Nair, Rico Andreas Haeuselmann, Riccardo Pisoni, Costas Bekas, Anna Iuliano, and Teodoro Laino. Predicting retrosynthetic pathways using transformer-based models and a hyper-graph exploration strategy. *Chemical Science*, 11(12):3316–3325, 2020.

[22] Igor V Tetko, Pavel Karpov, Ruud Van Deursen, and Guillaume Godin. State-of-the-art augmented nlp transformer models for direct and single-step retrosynthesis. *Nature communications*, 11(1):1–11, 2020.

[23] Umit V Ucak, Taek Kang, Junsu Ko, and Juyong Lee. Substructure-based neural machine translation for retrosynthetic prediction. *Journal of Cheminformatics*, 13(1):4, 2021.

[24] Vipul Mann and Venkat Venkatasubramanian. Predicting chemical reaction outcomes: A grammar ontology-based transformer framework. *AIChE Journal*, 67(3):e17190, 2021.

[25] Vipul Mann and Venkat Venkatasubramanian. A formal grammar-based machine learning approach for predicting reaction outcomes. In *2020 Virtual AIChE Annual Meeting*. AIChE, 2020.

[26] Ashish Vaswani, Noam Shazeer, Niki Parmar, Jakob Uszkoreit, Llion Jones, Aidan N Gomez, Ł ukasz Kaiser, and Illia Polosukhin. Attention is all you need. In I. Guyon, U. V. Luxburg, S. Bengio, H. Wallach, R. Fergus, S. Vishwanathan, and R. Garnett, editors, *Advances in Neural Information Processing Systems 30*, pages 5998–6008. Curran Associates, Inc., 2017.

[27] N. Chomsky. Three models for the description of language. *IRE Transactions on Information Theory*, 2(3):113–124, Sep. 1956.

[28] David Weininger. Smiles, a chemical language and information system. 1. introduction to methodology and encoding rules. *Journal of Chemical Information and Computer Sciences*, 28(1):31–36, 1988.

[29] C. E. Shannon. A mathematical theory of communication. *Bell System Technical Journal*, 27(3):379–423, 1948.

[30] D. Bonchev and N. Trinajstić. Chemical information theory: Structural aspects. *International Journal of Quantum Chemistry*, 22(S16):463–480, 1982.

[31] Jerry Chandler. An Introduction to the Foundations of Chemical Information Theory. Tarski–Lesniewski Logical Structures and the Organization of Natural Sorts and Kinds. *Information*, 8(1):15, jan 2017.

[32] Daniel J. Graham. Information and organic molecules: Structure considerations via integer statistics. *Journal of Chemical Information and Computer Sciences*, 42(2):215–221, 2002. PMID: 11911689.

[33] Roman F Nalewajski and Robert G Parr. Information Theory Thermodynamics of Molecules and Their Hirshfeld Fragments. 2001.

[34] Roman F. Nalewajski and Robert G. Parr. Information theory, atoms in molecules, and molecular similarity. *Proceedings of the National Academy of Sciences*, 97(16):8879–8882, 2000.

[35] Daniel Mark Lowe. *Extraction of chemical structures and reactions from the literature*. PhD thesis, University of Cambridge, 2012.

[36] Nadine Schneider, Nikolaus Stiefl, and Gregory A Landrum. What's what: The (nearly) definitive guide to reaction role assignment. *Journal of chemical information and modeling*, 56(12):2336–2346, 2016.

[37] Diederik P. Kingma and Jimmy Ba. Adam: A method for stochastic optimization, 2014.

[38] Matt J. Kusner, Brooks Paige, and José Miguel Hernández-Lobato. Grammar variational autoencoder. 2017.

[39] Kishore Papineni, Salim Roukos, Todd Ward, and Wei-Jing Zhu. Bleu: a method for automatic evaluation of machine translation. In *Proceedings of the 40th annual meeting of the Association for Computational Linguistics*, pages 311–318, 2002.

[40] Shuangjia Zheng, Jiahua Rao, Zhongyue Zhang, Jun Xu, and Yuedong Yang. Predicting retrosynthetic reactions using self-corrected transformer neural networks. *Journal of Chemical Information and Modeling*, 60(1):47–55, 2020. PMID: 31825611.